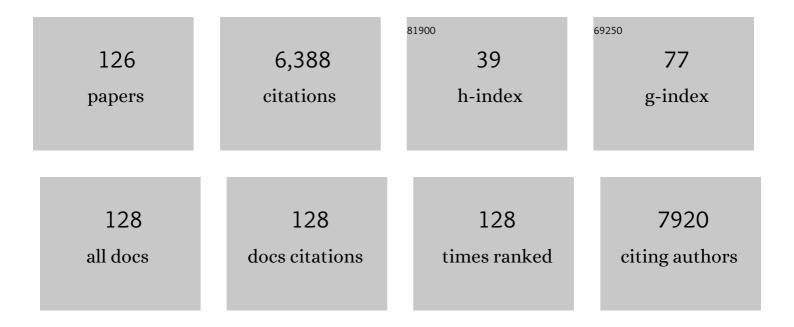
## Yu-Xiang Weng

List of Publications by Year in descending order

Source: https://exaly.com/author-pdf/7383295/publications.pdf Version: 2024-02-01



#	Article	IF	CITATIONS
1	Interstitial Pâ€Doped CdS with Longâ€Lived Photogenerated Electrons for Photocatalytic Water Splitting without Sacrificial Agents. Advanced Materials, 2018, 30, 1705941.	21.0	438
2	Isolated single atom cobalt in Bi3O4Br atomic layers to trigger efficient CO2 photoreduction. Nature Communications, 2019, 10, 2840.	12.8	327
3	Achieving overall water splitting using titanium dioxide-based photocatalysts of different phases. Energy and Environmental Science, 2015, 8, 2377-2382.	30.8	313
4	Defectâ€Tailoring Mediated Electron–Hole Separation in Singleâ€Unitâ€Cell Bi <sub>3</sub> O <sub>4</sub> Br Nanosheets for Boosting Photocatalytic Hydrogen Evolution and Nitrogen Fixation. Advanced Materials, 2019, 31, e1807576.	21.0	311
5	Direct Zâ€Scheme Heteroâ€phase Junction of Black/Red Phosphorus for Photocatalytic Water Splitting. Angewandte Chemie - International Edition, 2019, 58, 11791-11795.	13.8	301
6	Self-Retracting Motion of Graphite Microflakes. Physical Review Letters, 2008, 100, 067205.	7.8	193
7	Interfacial Electron Transfer between Fe(II)(CN)64-and TiO2Nanoparticles:Â Direct Electron Injection and Nonexponential Recombination. Journal of Physical Chemistry B, 1998, 102, 10208-10215.	2.6	181
8	Back Electron Transfer from TiO2 Nanoparticles to Felll(CN)63-:  Origin of Non-Single-Exponential and Particle Size Independent Dynamics. Journal of Physical Chemistry B, 2000, 104, 93-104.	2.6	168
9	Direct Z-Scheme Heterojunction of Semicoherent FAPbBr <sub>3</sub> /Bi <sub>2</sub> WO <sub>6</sub> Interface for Photoredox Reaction with Large Driving Force. ACS Nano, 2020, 14, 16689-16697.	14.6	167
10	Lightâ€Harvesting Systems Based on Organic Nanocrystals To Mimic Chlorosomes. Angewandte Chemie - International Edition, 2016, 55, 2759-2763.	13.8	151
11	Photo-assisted methanol synthesis via CO2 reduction under ambient pressure over plasmonic Cu/ZnO catalysts. Applied Catalysis B: Environmental, 2019, 250, 10-16.	20.2	142
12	Subâ€3 nm Ultrafine Cu <sub>2</sub> O for Visible Light Driven Nitrogen Fixation. Angewandte Chemie - International Edition, 2021, 60, 2554-2560.	13.8	134
13	Band Alignment and Controllable Electron Migration between Rutile and Anatase TiO2. Scientific Reports, 2015, 5, 11482.	3.3	131
14	Surface-Binding Forms of Carboxylic Groups on Nanoparticulate TiO2Surface Studied by the Interface-Sensitive Transient Triplet-State Molecular Probe. Journal of Physical Chemistry B, 2003, 107, 4356-4363.	2.6	129
15	Visible-Light-Mediated Methane Activation for Steam Methane Reforming under Mild Conditions: A Case Study of Rh/TiO <sub>2</sub> Catalysts. ACS Catalysis, 2018, 8, 7556-7565.	11.2	126
16	Metal@semiconductor core-shell nanocrystals with atomically organized interfaces for efficient hot electron-mediated photocatalysis. Nano Energy, 2018, 48, 44-52.	16.0	118
17	Cobalt nitride as a novel cocatalyst to boost photocatalytic CO2 reduction. Nano Energy, 2021, 79, 105429.	16.0	117
18	Constructing electron delocalization channels in covalent organic frameworks powering CO2 photoreduction in water. Applied Catalysis B: Environmental, 2020, 274, 119096.	20.2	113

#	Article	IF	CITATIONS
19	Unique Z-scheme carbonized polymer dots/Bi4O5Br2 hybrids for efficiently boosting photocatalytic CO2 reduction. Applied Catalysis B: Environmental, 2021, 293, 120182.	20.2	110
20	Surface Local Polarization Induced by Bismuthâ€Oxygen Vacancy Pairs Tuning Nonâ€Covalent Interaction for CO <sub>2</sub> Photoreduction. Advanced Energy Materials, 2021, 11, 2102389.	19.5	109
21	Direct Zâ€Scheme Heteroâ€phase Junction of Black/Red Phosphorus for Photocatalytic Water Splitting. Angewandte Chemie, 2019, 131, 11917-11921.	2.0	108
22	One‣tep Synthesis of Superbright Waterâ€Soluble Silicon Nanoparticles with Photoluminescence Quantum Yield Exceeding 80%. Advanced Materials Interfaces, 2015, 2, 1500360.	3.7	107
23	A Longâ€Lived Mononuclear Cyclopentadienyl Ruthenium Complex Grafted onto Anatase TiO <sub>2</sub> for Efficient CO <sub>2</sub> Photoreduction. Angewandte Chemie - International Edition, 2016, 55, 8314-8318.	13.8	96
24	Particle-Size-Dependent Distribution of Carboxylate Adsorption Sites on TiO2 Nanoparticle Surfaces: Insights into the Surface Modification of Nanostructured TiO2 Electrodes. Journal of Physical Chemistry B, 2004, 108, 15077-15083.	2.6	85
25	A Longâ€Lived Mononuclear Cyclopentadienyl Ruthenium Complex Grafted onto Anatase TiO <sub>2</sub> for Efficient CO <sub>2</sub> Photoreduction. Angewandte Chemie, 2016, 128, 8454-8458.	2.0	80
26	The Cyclophilin CYP20-2 Modulates the Conformation of BRASSINAZOLE-RESISTANT1, Which Binds the Promoter of FLOWERING LOCUS D to Regulate Flowering in Arabidopsis. Plant Cell, 2013, 25, 2504-2521.	6.6	78
27	Revealing the role of oxygen vacancies in bimetallic PbBiO2Br atomic layers for boosting photocatalytic CO2 conversion. Applied Catalysis B: Environmental, 2020, 277, 119170.	20.2	77
28	Challenges facing an understanding of the nature of low-energy excited states in photosynthesis. Biochimica Et Biophysica Acta - Bioenergetics, 2016, 1857, 1627-1640.	1.0	74
29	Black/red phosphorus quantum dots for photocatalytic water splitting: from a type I heterostructure to a Z-scheme system. Chemical Communications, 2019, 55, 12531-12534.	4.1	63
30	Deep Surface Trap Filling by Photoinduced Carriers and Interparticle Electron Transport Observed in TiO2 Nanocrystalline Film with Time-Resolved Visible and Mid-IR Transient Spectroscopies. Journal of Physical Chemistry C, 2007, 111, 3762-3769.	3.1	61
31	Ultrafast Energy Dissipation <i>via</i> Coupling with Internal and External Phonons in Two-Dimensional MoS <sub>2</sub> . ACS Nano, 2018, 12, 8961-8969.	14.6	61
32	Determination of Midgap State Energy Levels of an Anatase TiO <sub>2</sub> Nanocrystal Film by Nanosecond Transient Infrared Absorption – Excitation Energy Scanning Spectra. Journal of Physical Chemistry C, 2013, 117, 18863-18869.	3.1	55
33	Building of peculiar heterostructure of Ag/two-dimensional fullerene shell-WO3-x for enhanced photoelectrochemical performance. Applied Catalysis B: Environmental, 2018, 231, 381-390.	20.2	54
34	Photogenerated Intrinsic Free Carriers in Small-molecule Organic Semiconductors Visualized by Ultrafast Spectroscopy. Scientific Reports, 2015, 5, 17076.	3.3	52
35	White luminescent single-crystalline chlorinated graphene quantum dots. Nanoscale Horizons, 2020, 5, 928-933.	8.0	47
36	Broadly Tunable Plasmons in Doped Oxide Nanoparticles for Ultrafast and Broadband Mid-Infrared All-Optical Switching. ACS Nano, 2018, 12, 12770-12777.	14.6	46

#	Article	IF	CITATIONS
37	OsCIPK7 pointâ€mutation leads to conformation and kinaseâ€activity change for sensing cold response. Journal of Integrative Plant Biology, 2019, 61, 1194-1200.	8.5	46
38	The effects of pyridine derivative additives on interface processes at nanocrystalline TiO <sub>2</sub> thin film in dyeâ€sensitized solar cells. Surface and Interface Analysis, 2007, 39, 809-816.	1.8	45
39	Fluorescence Quenching in a Perylenetetracarboxylic Diimide Trimer. Journal of the American Chemical Society, 2009, 131, 30-31.	13.7	44
40	Porphyrin-Appended Europium(III) Bis(phthalocyaninato) Complexes: Synthesis, Characterization, and Photophysical Properties. Chemistry - A European Journal, 2007, 13, 4169-4177.	3.3	42
41	Ultrafast carrier transfer evidencing graphene electromagnetically enhanced ultrasensitive SERS in graphene/Ag-nanoparticles hybrid. Carbon, 2017, 122, 98-105.	10.3	40
42	Infrared Spectroscopic Discrimination between the Loop and α-Helices and Determination of the Loop Diffusion Kinetics by Temperature-Jump Time-Resolved Infrared Spectroscopy for Cytochrome c. Biophysical Journal, 2007, 93, 2756-2766.	0.5	39
43	Protein Structural Deformation Induced Lifetime Shortening of Photosynthetic Bacteria Light-Harvesting Complex LH2 Excited State. Biophysical Journal, 2005, 88, 4262-4273.	0.5	38
44	An organic nanowire waveguide exciton–polariton sub-microlaser and its photonic application. Journal of Materials Chemistry C, 2014, 2, 2773-2778.	5.5	38
45	Plasmon-induced hot electron transfer in Au–ZnO heterogeneous nanorods for enhanced SERS. Nanoscale, 2019, 11, 11782-11788.	5.6	38
46	Probing Nonequilibrium Dynamics of Photoexcited Polarons on a Metal-Oxide Surface with Atomic Precision. Physical Review Letters, 2020, 124, 206801.	7.8	37
47	Lightâ€Harvesting Systems Based on Organic Nanocrystals To Mimic Chlorosomes. Angewandte Chemie, 2016, 128, 2809-2813.	2.0	36
48	Direct Observation of Interfacial Charge Recombination to the Excited-Triplet State in All-trans-Retinoic Acid Sensitized TiO2Nanoparticles by Femtosecond Time-Resolved Difference Absorption Spectroscopy. Journal of Physical Chemistry B, 2003, 107, 13688-13697.	2.6	33
49	Ultrasensitive femtosecond time-resolved fluorescence spectroscopy for relaxation processes by using parametric amplification. Journal of the Optical Society of America B: Optical Physics, 2007, 24, 1633.	2.1	33
50	Single-photon level ultrafast all-optical switching. Applied Physics Letters, 2008, 92, .	3.3	33
51	Experimental Determination of Particle Size-Dependent Surface Charge Density for Silica Nanospheres. Journal of Physical Chemistry C, 2018, 122, 23764-23771.	3.1	33
52	Photoinduced Electron and Energy Transfer in Dyads of Porphyrin Dimer and Perylene Tetracarboxylic Diimide. ChemPhysChem, 2008, 9, 1409-1415.	2.1	32
53	Hydrogen Bond Interaction Promotes Flash Energy Transport at MXene-Solvent Interface. Journal of Physical Chemistry C, 2020, 124, 10306-10314.	3.1	32
54	TiO2/CdS composite hollow spheres with controlled synthesis of platinum on the internal wall for the efficient hydrogen evolution. International Journal of Hydrogen Energy, 2013, 38, 9065-9073.	7.1	31

#	Article	IF	CITATIONS
55	Boosting visible-light driven solar-fuel production over g-C3N4/tetra(4-carboxyphenyl)porphyrin iron(III) chloride hybrid photocatalyst via incorporation with carbon dots. Applied Catalysis B: Environmental, 2020, 265, 118595.	20.2	31
56	In Situ Switching of Photoinduced Electron Transfer Direction by Regulating the Redox State in Fullerene-Based Dyads. Journal of the American Chemical Society, 2020, 142, 4411-4418.	13.7	31
57	Ultrafast carrier and phonon dynamics in few-layer 2H–MoTe2. Journal of Chemical Physics, 2019, 151, 114704.	3.0	30
58	Dynamical and allosteric regulation of photoprotection in light harvesting complex II. Science China Chemistry, 2020, 63, 1121-1133.	8.2	29
59	Particle-Size-Dependent Hydrophilicity of TiO <sub>2</sub> Nanoparticles Characterized by Marcus Reorganization Energy of Interfacial Charge Recombination. Journal of Physical Chemistry C, 2008, 112, 8995-9000.	3.1	25
60	Transient spectrometer for near-IR fluorescence based on parametric frequency upconversion. Applied Physics Letters, 2006, 89, 061127.	3.3	24
61	Rules for Selecting Metal Cocatalyst Based on Charge Transfer and Separation Efficiency between ZnO Nanoparticles and Noble Metal Cocatalyst Ag/ Au/ Pt. ChemCatChem, 2020, 12, 3838-3842.	3.7	24
62	Highly efficient photocatalytic hydrogen production via porphyrin-fullerene supramolecular photocatalyst with donor-acceptor structure. Chemical Engineering Journal, 2022, 444, 136621.	12.7	22
63	Interfacial charge recombination via the triplet state? Mimicry of photoprotection in the photosynthetic process with a dye-sensitized TiO2 solar cell reaction. Chemical Physics Letters, 2002, 355, 294-300.	2.6	20
64	The effect mechanism of 4-ethoxy-2-methylpyridine as an electrolyte additive on the performance of dye-sensitized solar cell. Colloids and Surfaces A: Physicochemical and Engineering Aspects, 2008, 326, 42-47.	4.7	20
65	Effects of finite laser pulse width on two-dimensional electronic spectroscopy. Chemical Physics Letters, 2017, 667, 79-86.	2.6	20
66	Black Phosphorus Quantum Dots Modified CdS Nanowires with Efficient Charge Separation for Enhanced Photocatalytic H <sub>2</sub> Evolution. ChemCatChem, 2021, 13, 1355-1361.	3.7	20
67	Multi-channel lock-in amplifier assisted femtosecond time-resolved fluorescence non-collinear optical parametric amplification spectroscopy with efficient rejection of superfluorescence background. Review of Scientific Instruments, 2015, 86, 123113.	1.3	19
68	Effect of trap states on photocatalytic properties of boron-doped anatase TiO <sub>2</sub> microspheres studied by time-resolved infrared spectroscopy. Physical Chemistry Chemical Physics, 2019, 21, 4349-4358.	2.8	19
69	Cyclophilin OsCYP20â $\in 2$ with a novel variant integrates defense and cell elongation for chilling response in rice. New Phytologist, 2020, 225, 2453-2467.	7.3	19
70	Unique Cation Exchange in Nanocrystal Matrix via Surface Vacancy Engineering Overcoming Chemical Kinetic Energy Barriers. CheM, 2020, 6, 3086-3099.	11.7	18
71	Observation of delayed fluorescence in CdSxSe1â^'x nanobelts by femtosecond time-resolved fluorescence spectroscopy. Applied Physics Letters, 2008, 92, .	3.3	17
72	Coupling of multi-vibrational modes in bacteriochlorophyll a in solution observed with 2D electronic spectroscopy. Chemical Physics Letters, 2017, 683, 591-597.	2.6	17

#	Article	IF	CITATIONS
73	Simulation of the Two-Dimensional Electronic Spectroscopy and Energy Transfer Dynamics of Light-Harvesting Complex II at Ambient Temperature. Journal of Physical Chemistry B, 2018, 122, 4642-4652.	2.6	17
74	Characterization of ultra-weak fluorescence using picosecond non-collinear optical parametric amplifier. Optics Communications, 2009, 282, 1884-1887.	2.1	16
75	Observation of the hot-phonon effect in monolayer MoS <sub>2</sub> . Nanotechnology, 2020, 31, 235712.	2.6	16
76	Highly Efficient and Selective Aerobic Oxidation of Cinnamyl Alcohol under Visible Light over Pt-Loaded NaNbO <sub>3</sub> Enriched with Oxygen Vacancies by Ni Doping. ACS Sustainable Chemistry and Engineering, 2021, 9, 5422-5429.	6.7	14
77	Effect of laser intensity on the determination of intermolecular electron transfer rate constants—Observation of Marcus inverted region in photoinduced back electron transfer reactions. Journal of Chemical Physics, 1998, 109, 5948-5956.	3.0	13
78	Prolonged Excited-State Lifetime of Porphyrin Due to the Addition of Colloidal SiO2to Triton X-100 Micelles. Langmuir, 2004, 20, 1582-1586.	3.5	13
79	Intermolecular Hydrogen Bonds Formed Between Amino Acid Molecules in Aqueous Solution Investigated by Temperature-jump Nanosecond Time-resolved Transient Mid-IR Spectroscopy. Chinese Journal of Chemical Physics, 2007, 20, 461-467.	1.3	13
80	Ultrafast energy transfer pathways in R-phycoerythrin from Polysiphonia urceolata. Photosynthesis Research, 2012, 111, 81-86.	2.9	13
81	Vibrational Relaxation Dynamics of a Semiconductor Copper(I) Thiocyanate (CuSCN) Film as a Hole-Transporting Layer. Journal of Physical Chemistry Letters, 2020, 11, 548-555.	4.6	13
82	Subâ€3 nm Ultrafine Cu 2 O for Visible Light Driven Nitrogen Fixation. Angewandte Chemie, 2021, 133, 2584-2590.	2.0	13
83	Noncollinear optical parametric amplifier based femtosecond time-resolved transient fluorescence spectra: characterization and correction. Journal of the Optical Society of America B: Optical Physics, 2009, 26, 1627.	2.1	12
84	Thermal-Induced Dissociation and Unfolding of Homodimeric DsbC Revealed by Temperature-Jump Time-Resolved Infrared Spectra. Biophysical Journal, 2009, 97, 2811-2819.	0.5	12
85	Photo Retro-Diels–Alder Reactions. Journal of Physical Chemistry A, 2011, 115, 8093-8099.	2.5	12
86	Shell Thickness Dependence of the Plasmon-Induced Hot-Electron Injection Process in Au@CdS Core–Shell Nanocrystals. Journal of Physical Chemistry C, 2021, 125, 19906-19913.	3.1	12
87	Photosynthetic Bacterial Light-Harvesting Antenna Complexes Adsorbed on Silica Nanoparticles Revealed by Silica Shell-Isolated Au Nanoparticle-Enhanced Raman Spectroscopy. Journal of Physical Chemistry C, 2012, 116, 6993-6999.	3.1	11
88	Thermal-triggerd Proteinquake Leads to Disassembly of DegP Hexamer as an Imperative Activation Step. Scientific Reports, 2014, 4, 4834.	3.3	11
89	Electronic State-Resolved Multimode-Coupled Vibrational Wavepackets in Oxazine 720 by Two-Dimensional Electronic Spectroscopy. Journal of Physical Chemistry A, 2020, 124, 9333-9342.	2.5	11
90	A Supercomplex, of Approximately 720 kDa and Composed of Both Photosystem Reaction Centers, Dissipates Excess Energy by PSI in Green Macroalgae Under Salt Stress. Plant and Cell Physiology, 2019, 60, 166-175.	3.1	9

#	Article	IF	CITATIONS
91	Correction of spectral distortion in two-dimensional electronic spectroscopy arising from the wedge-based delay line. Optics Express, 2019, 27, 15474.	3.4	9
92	Amphiphilic porphyrins in reverse micelles: the influence of the molar ratio of water to surfactant and side-chain length on their triplet-state lifetimes. A case studyElectronic supplementary information (ESI) available: Further experimental details. See http://www.rsc.org/suppdata/cp/b3/b302607h/. Physical Chemistry Chemical Physics, 2003, 5, 3660.	2.8	8
93	Photoinduced Charge Recombination at Dye-Sensitized Individual TiO2Nanoparticles and Its Application in Probe for the Local Polarity Change around the Nanoparticle in Solution. Journal of Physical Chemistry C, 2007, 111, 4567-4577.	3.1	8
94	Construction of the Apparatus for Two Dimensional Electronic Spectroscopy and Characterization of the Instrument. Chinese Journal of Chemical Physics, 2015, 28, 509-517.	1.3	8
95	Influence of Water in the Photogeneration and Properties of a Bifunctional Quinone Methide. Journal of Physical Chemistry B, 2016, 120, 11132-11141.	2.6	8
96	Observation of the Polaron Excited State in a Single-Crystal ZnO. Journal of Physical Chemistry C, 2021, 125, 10274-10283.	3.1	8
97	Determination of the detection limit for a noncollinear optical parametric amplification-gated femtosecond time-resolved fluorescence spectrometerâ $\in$ "Reply to the Comment on â $\in$ œUltrasensitive femtosecond time-resolved fluorescence spectroscopy for relaxation processes by using parametric amplificationâ $\in$ lournal of the Optical Society of America B: Optical Physics. 2008. 25. 1627.	2.1	7
98	Filamentary resistance switching in phthalocyanine thin films observed by electroluminescence. Applied Physics Letters, 2015, 106, .	3.3	7
99	Detection of Electronic Coherence via Two-Dimensional Electronic Spectroscopy in Condensed Phase. Chinese Journal of Chemical Physics, 2018, 31, 135-151.	1.3	7
100	Vibrational and vibronic coherences in the energy transfer process of light-harvesting complex II revealed by two-dimensional electronic spectroscopy. Journal of Chemical Physics, 2022, 156, 125101.	3.0	7
101	Direct Observation of Mass Transfer at Solidâ^'Liquid Interface by Laser Flash Photolysis of the Interface Probe Molecules. Journal of Physical Chemistry B, 2000, 104, 7713-7724.	2.6	6
102	Nonlinear chirp effect introduced by Kerr medium as optical switches in ultrafast time-resolved measurements. Optics Letters, 2009, 34, 1117.	3.3	6
103	Coherent photon interference elimination and spectral correction in femtosecond time-resolved fluorescence non-collinear optical parametric amplification spectroscopy. Review of Scientific Instruments, 2013, 84, 073105.	1.3	6
104	Transitional Process of Ploy(N-isopropylacrylamide) in Deuterated Solution. Chinese Journal of Chemical Physics, 2009, 22, 447-452.	1.3	5
105	Ultrafast Energy Transfer in Artificial Antenna Molecule Measured by Transient Fluorescence Spectroscopy. Chinese Journal of Chemical Physics, 2011, 24, 253-255.	1.3	5
106	A Q-switched Ho:YAG laser assisted nanosecond time-resolved T-jump transient mid-IR absorbance spectroscopy with high sensitivity. Review of Scientific Instruments, 2015, 86, 053105.	1.3	5
107	A transient molecular probe for characterizing the surface properties of TiO2 nanoparticle in colloidal solution. Science and Technology of Advanced Materials, 2005, 6, 867-872.	6.1	4
108	Infrared Absorption Intensity Analysis as a New Tool for Investigation of Salt Effect on Proteins. Chinese Journal of Chemical Physics, 2009, 22, 556-562.	1.3	4

#	Article	IF	CITATIONS
109	Spatial distribution of carrier-envelope phase for femtosecond pulsed laser beam profile determined by asymmetric spectral interferometry. Optics Letters, 2010, 35, 2275.	3.3	4
110	Carrier Recombination-Incited Substrate Vibrations after Pulsed UV-Laser Photolysis of TiO <sub>2</sub> Thin Single-Crystal Plate and Nanoparticle Films. Applied Spectroscopy, 2013, 67, 506-512.	2.2	4
111	Determining Quasiparticle Bandgap of Two-Dimensional Transition Metal Dichalcogenides by Observation of Hot Carrier Relaxation Dynamics. Journal of Physical Chemistry Letters, 2021, 12, 585-591.	4.6	4
112	Interference pattern generation and simulation in the single beam of a white light continuum. Science China: Physics, Mechanics and Astronomy, 2010, 53, 1060-1064.	5.1	3
113	Silicon Nanoparticles: One‣tep Synthesis of Superbright Water‣oluble Silicon Nanoparticles with Photoluminescence Quantum Yield Exceeding 80% (Adv. Mater. Interfaces 16/2015). Advanced Materials Interfaces, 2015, 2, .	3.7	3
114	Measuring the carrier dynamics of photocatalyst micrograins using the Christiansen effect. Journal of Chemical Physics, 2017, 146, 234202.	3.0	3
115	Real-time observation of vibrational quantum beat in condensed phase by 20 fs time-resolved spectroscopy. Chinese Science Bulletin, 2012, 57, 2895-2898.	0.7	3
116	The mechanism for thermal-enhanced chaperone-like activity of $\hat{I}\pm$ -crystallin against UV irradiation-induced aggregation of $\hat{I}^3D$ -crystallin. Biophysical Journal, 2022, , .	0.5	3
117	Femtosecond time-resolved fluorescence non-collinear optical parametric amplification spectroscopy. Scientia Sinica Chimica, 2013, 43, 1713-1729.	0.4	2
118	Efficient Longâ€Range Triplet Exciton Transport by Metal–Metal Interaction at Room Temperature. Angewandte Chemie, 0, , .	2.0	2
119	Temporal Evolution of Photothermal-Induced Rayleigh Wave and Plate Deformation as an Interference in the Transient Kinetics of Photoinduced Carrier Recombination of a Rutile Titanium Dioxide Single Crystal. Applied Spectroscopy, 2014, 68, 1374-1380.	2.2	1
120	C60-modified mixed (phthalocyaninato)(porphyrinato) yttrium(III) double-decker complex: Synthesis, characterization, and photophysical properties. Dyes and Pigments, 2014, 102, 257-262.	3.7	1
121	Synchronous Measurement of Ultrafast Anisotropy Decay of the B850 in Bacterial LH2 Complex. Chinese Physics Letters, 2015, 32, 023101.	3.3	1
122	Spectrum Correction in Study of Solvation Dynamics by Fluorescence Non-collinear Optical Parametric Amplification Spectroscopy. Chinese Journal of Chemical Physics, 2016, 29, 147-150.	1.3	1
123	Lasing dynamics study by femtosecond time-resolved fluorescence non-collinear optical parametric amplification spectroscopy. Chinese Physics B, 2016, 25, 054207.	1.4	1
124	Structure-dependent wavelike energy transfer on pigment rings of individual light-harvesting-2 complexes from photosynthetic bacteria. Physical Review E, 2010, 81, 041917.	2.1	0
125	New method for fast morphological characterization of organic polycrystalline films by polarized optical microscopy. Chinese Physics B, 2015, 24, 076803.	1.4	0
126	Structural Reorganization of a Synthetic Mimic of the Oxygen-Evolving Center in Multiple Redox Transitions Revealed by Electrochemical FTIR Spectra. Journal of Physical Chemistry Letters, 2021, 12, 9830-9839.	4.6	0